

1           **PhyKIT: a UNIX shell toolkit for processing and analyzing phylogenomic data**

2

3   Jacob L. Steenwyk<sup>1,\*</sup>, Thomas J. Buida III<sup>2</sup>, Abigail L. Labella<sup>1</sup>, Yuanning Li<sup>1</sup>, Xing-Xing  
4   Shen<sup>3</sup>, & Antonis Rokas<sup>1,\*</sup>

5

6   <sup>1</sup> Vanderbilt University, Department of Biological Sciences, VU Station B #35-1634, Nashville,  
7   TN 37235, United States of America

8   <sup>2</sup> 9 City Place #312, Nashville, TN 37209, United States of America

9   <sup>3</sup> Ministry of Agriculture Key Lab of Molecular Biology of Crop Pathogens and Insects, Institute  
10   of Insect Sciences, Zhejiang University, Hangzhou 310058, China

11

12   \*Correspondence should be addressed to: [jacob.steenwyk@vanderbilt.edu](mailto:jacob.steenwyk@vanderbilt.edu) or  
13   [antonis.rokas@vanderbilt.edu](mailto:antonis.rokas@vanderbilt.edu)

14

15   **ORCiDs**

16   J.L. Steenwyk: 0000-0002-8436-595X

17   T.J. Buida III: 0000-0001-9367-6189

18   Abigail L. Labella: 0000-0003-0068-6703

19   Y. Li: 0000-0002-2206-5804

20   X.-X. Shen: 0000-0001-5765-1419

21   A. Rokas: 0000-0002-7248-6551

22

23   **Running title:** PhyKIT: a toolkit for examining phylogenomic datasets

24 **Keywords:** molecular phylogenetics, phylogenomics, multiple sequence alignment, phylogenetic  
25 signal, network, gene-gene covariation, evolutionary rate, polytomy, tree distance

26

27 **Abstract**

28 Diverse disciplines in biology process and analyze multiple sequence alignments (MSAs) and  
29 phylogenetic trees to evaluate their information content, infer evolutionary events and processes,  
30 and predict gene function. However, automated processing of MSAs and trees remains a  
31 challenge due to the lack of a unified toolkit. To fill this gap, we introduce PhyKIT, a toolkit for  
32 the UNIX shell environment with 30 functions that process MSAs and trees, including but not  
33 limited to estimation of mutation rate, evaluation of sequence composition biases, calculation of  
34 the degree of violation of a molecular clock, and collapsing bipartitions (internal branches) with  
35 low support. To demonstrate the utility of PhyKIT, we detail three use cases: (1) summarizing  
36 information content in MSAs and phylogenetic trees for diagnosing potential biases in sequence  
37 or tree data; (2) evaluating gene-gene covariation of evolutionary rates to identify functional  
38 relationships, including novel ones, among genes; and (3) identify lack of resolution events or  
39 polytomies in phylogenetic trees, which are suggestive of rapid radiation events or lack of data.  
40 We anticipate PhyKIT will be useful for processing, examining, and deriving biological meaning  
41 from increasingly large phylogenomic datasets. PhyKIT is freely available on GitHub  
42 (<https://github.com/JLSteenwyk/PhyKIT>) and documentation including user tutorials are  
43 available online (<https://jlsteenwyk.com/PhyKIT>).

## 44 **Introduction**

45 Multiple sequence alignments (MSAs) and phylogenetic trees are widely used in numerous  
46 disciplines, including bioinformatics, evolutionary biology, molecular biology, and structural  
47 biology. As a result, the development of user-friendly software that enables biologists to process  
48 and analyze MSAs and phylogenetic trees is an active area of research (Kapli *et al.* 2020).

49  
50 In recent years, numerous methods have proven useful for diagnosing potential biases and  
51 inferring biological events in genome-scale phylogenetic (or phylogenomic) datasets. For  
52 example, methods that evaluate sequence composition biases in MSAs (Phillips and Penny  
53 2003), signatures of clock-like evolution in phylogenetic trees (Liu *et al.* 2017), phylogenetic  
54 treeness (Lanyon 1988; Phillips and Penny 2003), taxa whose long branches may cause variation  
55 in their placement on phylogenetic trees (Struck 2014), and others have assisted in summarizing  
56 the information content in phylogenomic datasets and improved phylogenetic inference  
57 (Felsenstein 1978; Philippe *et al.* 2011; Salichos and Rokas 2013; Doyle *et al.* 2015; Liu *et al.*  
58 2017; Smith *et al.* 2018; Walker *et al.* 2019).

59  
60 Other methodological innovations include identifying significant gene-gene covariation of  
61 evolutionary rate, which has been shown to accurately and sensitively identify genes that have  
62 shared functions, are co-expressed, and/or are part of the same multimeric complexes (Sato *et al.*  
63 2005; Clark *et al.* 2012). Furthermore, gene-gene covariation serves as a powerful evolution-  
64 based genetic screen for predicting gene function (Brunette *et al.* 2019). Lastly, a recently  
65 developed method has enabled the identification of unresolved internal branches or polytomies in  
66 species trees (Sayyari and Mirarab 2018; One Thousand Plant Transcriptomes Initiative 2019);

67 such branches can stem from rapid radiation events or from lack of data (Rokas and Carroll  
68 2006).

69

70 Despite the wealth of information in MSAs and phylogenetic trees, there is a dearth of tools,  
71 especially ones that allow to conduct these analyses in a unified framework. For example, to  
72 utilize the functions mentioned in the previous paragraphs, a combination of web-server  
73 applications, ‘hard-coded’ scripts available through numerous repositories and supplementary  
74 material, standalone software, and/or extensive programming in languages including R, Python,  
75 or C is currently required (Cock *et al.* 2009; Junier and Zdobnov 2010; Revell 2012; Talevich *et*  
76 *al.* 2012; Struck 2014; Kück and Longo 2014; Wolfe and Clark 2015; One Thousand Plant  
77 Transcriptomes Initiative 2019). As a result, integrating these functions into bioinformatic  
78 pipelines is challenging, reducing their accessibility to the scientific community.

79

80 To facilitate the integration of these methods into bioinformatic pipelines, we introduce PhyKIT,  
81 a UNIX shell toolkit with 30 functions (Table 1) with broad utility for analyzing and processing  
82 MSAs and phylogenetic trees. Current functions implemented in PhyKIT include measuring  
83 topological similarity of phylogenetic trees, creating codon-based MSAs, concatenating sets of  
84 MSAs into phylogenomic datasets, editing and/or viewing alignments and phylogenetic trees,  
85 and identifying putatively spurious homologs in MSAs. We highlight three uses of PhyKIT: (1)  
86 calculating diverse statistics that summarize the information content and potential biases (e.g.,  
87 sequence- or phylogeny-based biases) in MSAs and phylogenetic trees; (2) creating a gene-gene  
88 covariation network of evolutionary rates; and (3) inferring the presence of polytomies from

89 phylogenomic data. The diverse functions implemented in PhyKIT will likely be of interest to  
90 bioinformaticians, molecular biologists, evolutionary biologists, and others.

91

## 92 **Materials and Methods**

93 PhyKIT is a command line tool for the UNIX shell environment written in the Python  
94 programming language (<https://www.python.org/>). PhyKIT requires few dependencies  
95 (Biopython (Cock *et al.* 2009) and SciPy (Virtanen *et al.* 2020)) making it user-friendly to install  
96 and integrate into existing bioinformatic pipelines. Furthermore, the online documentation of  
97 PhyKIT comes complete with tutorials that detail how to use various functions. Lastly, PhyKIT  
98 is modularly designed to allow straightforward integration of additional functions in future  
99 versions.

100

101 PhyKIT has 30 different functions that help process and analyze MSAs and phylogenetic trees  
102 (Table 1). The 30 functions can be grouped into broad categories that assist in conducting  
103 analyses of MSAs and phylogenies or in processing/editing them. For example, “analysis”  
104 functions help examine information content biases, gene-gene covariation, and polytomies in  
105 phylogenomic datasets; “processing/editing” functions help prune tips from phylogenies,  
106 collapse poorly supported bipartitions in phylogenetic trees, concatenate sets of MSAs into a  
107 single data matrix, or create codon-based alignments from protein alignments and their  
108 corresponding nucleotide sequences.

109

110 Detailed information about each one of PhyKIT’s functions and tutorials for using the software  
111 can be found in the online documentation (<https://jlsteenwyk.com/PhyKIT>). Here, we focus on

112 three specific groups of functions implemented in PhyKIT that enable researchers to summarize  
113 information content in phylogenomic datasets, create gene-gene evolutionary rate covariation  
114 networks, and identifying polytomies in phylogenomic data.

115

### 116 **Evaluating information content and biases in phylogenomic datasets**

117 MSAs and phylogenetic trees are frequently examined to evaluate their information content and  
118 potential biases in characteristics such as sequence composition or branch lengths (Phillips and  
119 Penny 2003; Philippe *et al.* 2011; Struck 2014; Doyle *et al.* 2015; Shen *et al.* 2016a; Liu *et al.*  
120 2017; Smith *et al.* 2018). PhyKIT implements numerous functions for doing so. Here, we  
121 demonstrate the application of 14 functions:

122 (1) *Alignment length*. The length of a multiple sequence alignment, which is associated with  
123 robust bipartition support and tree accuracy (Shen *et al.* 2016a; Walker *et al.* 2019);

124 (2) *Alignment length with no gaps*. The length of a multiple sequence alignment after excluding  
125 sites with gaps, which is associated with robust bipartition support and tree accuracy (Shen *et al.*  
126 2016a);

127 (3) *Degree of violation of a molecular clock (DVMC)*. A metric used to determine the clock-like  
128 evolution of a gene using the standard deviation of branch lengths for a single gene tree (Liu *et*  
129 *al.* 2017). DVMC is calculated using the following formula:

$$DVMC = \sqrt{\frac{1}{N-1} \sum_{j=1}^N (i_j - \bar{i})^2}$$

130 where  $N$  represents the number of tips in a phylogenetic tree,  $i_j$  being the distance between the  
131 root of the tree and species  $j$ , and  $\bar{i}$  represents the average root to tip distance. DVMC can be  
132 used to identify genes with clock-like evolution for divergence time estimation (Liu *et al.* 2017);

133 (4) *Internal branch lengths*. Summary statistics of internal branch lengths in a phylogenetic tree  
134 are reported including mean, median, 25<sup>th</sup> percentile, 75<sup>th</sup> percentile, minimum, maximum,  
135 standard deviation, and variance values. Examination of internal branch lengths is useful in  
136 evaluating phylogenetic tree shape;

137 (5) *Long branch score*. A metric that examines the degree of taxon-specific long branch  
138 attraction (Struck 2014; Weigert *et al.* 2014). Long branch scores of individual taxa are  
139 calculated using the following formula:

$$LB_i = \left( \frac{\overline{PD}_i}{\overline{PD}_{all}} - 1 \right) \times 100$$

140 where  $\overline{PD}_i$  represents the average pairwise patristic distance of taxon  $i$  to all other taxa,  $\overline{PD}_{all}$   
141 represents the average patristic distance across all taxa, and  $LB_i$  represents the long branch score  
142 of taxon  $i$ . Long branch scores can be used to evaluate heterogeneity in tip-to-root distances and  
143 identify taxa that may be susceptible to long branch attraction;

144 (6) *Pairwise identity*. Pairwise identity is a crude approximation of the evolutionary rate of a  
145 gene and is calculated by determining the average number of sites in an MSA that are the same  
146 character state between all pairwise combinations of taxa. This can be used to group genes based  
147 on their evolutionary rates (e.g., faster-evolving genes vs. slower-evolving ones) (Chen *et al.*  
148 2017);

149 (7) *Patristic distances*. Patristic distances refer to all distances between all pairwise combinations  
150 of tips in a phylogenetic tree (Fourment and Gibbs 2006), which can be used to evaluate the rate  
151 of evolution in gene trees or taxon sampling density in species trees;

152 (8) *Parsimony-informative sites*. Parsimony-informative sites are those sites in an MSA that have  
153 a least two character states (excluding gaps) that occur at least twice (Kumar *et al.* 2016); the

154 number of parsimony-informative sites is associated with robust bipartition support and tree  
155 accuracy (Shen *et al.* 2016a; Steenwyk *et al.* 2020);  
156 (9) *Variable sites*. Variable sites are those sites in an MSA that contain at least two different  
157 character states (excluding gaps) (Kumar *et al.* 2016); the number of variable sites is associated  
158 with robust bipartition support and tree accuracy (Shen *et al.* 2016a);  
159 (10) *Relative composition variability*. Relative composition variability is the average variability  
160 in the sequence composition among taxa in an MSA. Relative composition variability is  
161 calculated using the following formula:

$$\text{Relative composition variability} = \sum_{i=1}^c \sum_{j=1}^n \frac{|c_{ij} - \bar{c}_i|}{s \times n}$$

162 where  $c$  is the number of different character states per sequence type,  $n$  is the number of taxa in  
163 an MSA,  $c_{ij}$  is the number of occurrences of the  $i$ th character state for the  $j$ th taxon,  $\bar{c}_i$  is the  
164 average number of the  $i$ th  $c$  character state across  $n$  taxa, and  $s$  refers to the total number of sites  
165 (characters) in an MSA. Relative composition variability can be used to evaluate potential  
166 sequence composition biases in MSAs, which in turn violate assumptions of site composition  
167 homogeneity in standard models of sequence evolution (Phillips and Penny 2003);  
168 (11) *Saturation*. Saturation refers to when an MSA contains many sites that have experienced  
169 multiple substitutions in individual taxa. Saturation is estimated from the slope of the regression  
170 line between patristic distances and pairwise identities. Saturated MSAs have reduced  
171 phylogenetic information and can result in issues of long branch attraction (Lake 1991; Philippe  
172 *et al.* 2011);  
173 (12) *Total tree length*. Total tree length refers to the sum of internal and terminal branch lengths  
174 and is calculated using the following formula:



$$\text{total tree length} = \sum_{i=1}^a l_i + \sum_{j=1}^b l_j$$

175

176 Where  $l_i$  is the branch length of the  $i$ th branch of  $a$  internal branches and  $l_j$  is the branch length of  
177 the  $j$ th branch of  $b$  terminal branches. Total tree length measures the inferred total amount or rate  
178 of evolutionary change in a phylogenetic tree;

179 (13) *Treeness*. Treeness (also referred to as stemminess) is a measure of the inferred relative  
180 amount or rate of evolutionary change that has taken place on internal branches of a phylogenetic  
181 tree (Lanyon 1988; Phillips and Penny 2003) and is calculated using the following formula:

$$\text{treeness} = \sum_{u=1}^b \frac{l_u}{l_t}$$

182 where  $l_u$  is the branch length of the  $u$ th branch of  $b$  internal branches, and  $l_t$  refers to the total  
183 branch length of the phylogenetic tree. Treeness can be used to evaluate how much of the total  
184 tree length is observed among internal branches;

185 (14) *Treeness divided by relative composition variability*. This function combines two metrics to  
186 measure both composition bias and other biases that may negatively influence phylogenetic  
187 inference. High treeness divided by relative composition variability values have been shown to  
188 be less susceptible to sequence composition biases and are associated with robust bipartition  
189 support and tree accuracy (Phillips and Penny 2003; Shen *et al.* 2016a).

190

### 191 **Calculating gene-gene evolutionary rate covariation or coevolution**

192 Genes that share similar rates of evolution through speciation events (or coevolve) tend to have  
193 similar functions, expression levels, or are parts of the same multimeric complexes (Sato *et al.*  
194 2005; Clark *et al.* 2012). Thus, identifying significant coevolution between genes (i.e.,

195 identifying genes that are significantly correlated in their evolutionary rates across speciation  
196 events) can be a powerful evolution-based screen to determine gene function (Brunette *et al.*  
197 2019).

198

199 To measure gene-gene evolutionary rate covariation, PhyKIT implements the mirror tree method  
200 (Pazos and Valencia 2001; Sato *et al.* 2005), which examines whether two trees have correlated  
201 branch lengths. Specifically, PhyKIT calculates the Pearson correlation coefficient between  
202 branch lengths in two phylogenetic trees that share the same tips and topology. To account for  
203 differences in taxon representation between the two trees, PhyKIT first automatically determines  
204 which taxa are shared and prunes one or both such that the same set of taxa is present in both  
205 trees. PhyKIT requires that the two input trees have the same topology, which is typically the  
206 species tree topology inferred from whole genome or proteome data. Thus, the user will typically  
207 first estimate a gene's branch lengths by constraining the topology to match that of the species  
208 tree. When running this function, users should be aware that many biological factors, such as  
209 horizontal transfer (Doolittle and Baptiste 2007), incomplete lineage sorting (Degnan and Salter  
210 2005), and introgression / hybridization (Sang and Zhong 2000), can lead to gene histories that  
211 deviate from the species tree. In these cases, constraining a gene's history to match that of a  
212 species may lead to errors in the covariation analysis.

213

214 Due to factors including time since speciation and mutation rate, correlations between  
215 uncorrected branch lengths result in a high frequency of false positive correlations (Sato *et al.*  
216 2005; Clark *et al.* 2012; Chikina *et al.* 2016). To ameliorate the influence of these factors,  
217 PhyKIT first transforms branch lengths into relative rates. To do so, branch lengths are corrected

218 by dividing the branch length in the gene tree by the corresponding branch length in the species  
219 tree. Previous work revealed that one or a few outlier branch length values can be responsible for  
220 false positive correlations and should be removed prior to analysis (Clark *et al.* 2012). Thus,  
221 PhyKIT removes outlier data points defined as having corrected branch lengths greater than five  
222 (i.e., removing gene tree branch lengths that are five or more times greater than their  
223 corresponding species tree branch lengths). Lastly, values are converted into relative rates using  
224 a Z-transformation. The resulting relative rates are used when calculating Pearson correlation  
225 coefficients.

226

### 227 **Identifying polytomies in phylogenomic data**

228 Rapid radiations or diversification events have occurred throughout the tree of life including  
229 among mammals, birds, plants, and fungi (Jarvis *et al.* 2014; Liu *et al.* 2017; One Thousand  
230 Plant Transcriptomes Initiative 2019; Li *et al.* 2020). Polytomies correspond to internal branches  
231 whose length is 0 (or statistically indistinguishable from 0) and can be driven either by biological  
232 (e.g., rapid radiations) or analytical (e.g., low amount of data) factors. Thus, polytomies are  
233 useful for inferring rapid radiation or diversification events and exploring incongruence in  
234 phylogenies (Sayyari and Mirarab 2018; One Thousand Plant Transcriptomes Initiative 2019; Li  
235 *et al.* 2020).

236

237 To identify polytomies, a modified approach to a previous strategy was implemented (Sayyari  
238 and Mirarab 2018). More specifically, the support for three alternative topologies is calculated  
239 among all gene trees from a phylogenomic dataset. For example, in species tree  $((A,B),C), D$ );, if  
240 examining the presence of a polytomy at the ancestral bipartition of tips  $A, B$ , and  $C$ , PhyKIT

241 will determine the number of gene trees that support  $((A,B),C)$ ;,  $((A,C),B)$ ;, and  $((B,C),A)$ ;; using  
242 the rooted gene trees provided by the user. Equal support for the three topologies (i.e., the  
243 presence of a polytomy) among a set of gene trees is assessed using a Chi-squared test. Failing to  
244 reject the null hypothesis is indicative of a polytomy (Sayyari and Mirarab 2018). Note that this  
245 approach is distinct from the approach of Sayyari and Mirarab to identify polytomies because  
246 PhyKIT uses a gene-based signal rather than a quartet-based signal. The difference between the  
247 two methods is that each gene contributes equally to the inference of a polytomy when a gene-  
248 based signal is used, whereas genes with greater taxon representation (which contain a greater  
249 number of quartets) will contribute a greater signal during polytomy identification when a  
250 quartet-based signal is used.

251

## 252 **Results and Discussion**

253 We outline three example uses of PhyKIT: 1) summarizing information content and identifying  
254 potential biases in animal, plant, yeast, and filamentous fungal phylogenomic datasets (Shen *et al.*  
255 *et al.* 2016b; Steenwyk *et al.* 2019; Laumer *et al.* 2019; One Thousand Plant Transcriptomes  
256 Initiative 2019), 2) constructing a network of significant gene-gene covariation, which reveals  
257 genes of shared functions from empirical data spanning ~550 million years of evolution among  
258 fungi (Shen *et al.* 2020), and 3) illustrating how to identify polytomies using simulated and  
259 empirical data (Steenwyk *et al.* 2019).

260

### 261 **Summarizing information content and biases in phylogenomic data**

262 Examining information content in phylogenomic datasets can help diagnose potential biases that  
263 stem from low signal-to-noise ratios, multiple substitutions, non-clocklike evolution, and other

264 biological or analytical factors. To demonstrate the utility of PhyKIT to summarize the  
265 information content in phylogenomic datasets, we calculated 14 different metrics known to help  
266 diagnose potential biases in phylogenomic datasets or be associated with accurate and well  
267 supported phylogenetic inferences (Felsenstein 1978; Phillips and Penny 2003; Philippe *et al.*  
268 2011; Struck 2014; Doyle *et al.* 2015; Shen *et al.* 2016a; Liu *et al.* 2017; Smith *et al.* 2018) using  
269 four empirical phylogenomic datasets from animals (201 tips; 2,891 genes) (Laumer *et al.* 2019),  
270 budding yeast (332 taxa; 2,408 genes) (Shen *et al.* 2018), filamentous fungi (93 taxa; 1,668  
271 genes) (Steenwyk *et al.* 2019), and plants (1,124 taxa; 403 genes) (One Thousand Plant  
272 Transcriptomes Initiative 2019) (Figure 1, Table 1).

273

274 Examination of the distributions of the values of the 14 different metrics revealed inter- and  
275 intra-dataset heterogeneity (Figure 1). For example, inter-dataset heterogeneity was observed  
276 among animal and plant datasets, which had the lowest and highest average pairwise identity  
277 across alignments, respectively; intra-dataset heterogeneity was observed in the uniform  
278 distribution of pairwise identities in the budding yeast datasets. Similarly, inter-dataset  
279 heterogeneity was observed in estimates of saturation where the budding yeast and filamentous  
280 fungal MSAs were less saturated by multiple substitutions than the plant and animal datasets;  
281 intra-data heterogeneity was also observed in all four datasets. Varying degrees of inter- and  
282 intra-dataset heterogeneity was observed for other information content statistics, which may be  
283 due biological (e.g., mutation rate) or analytical factors (e.g., taxon sampling, distinct alignment,  
284 trimming, and tree inference strategies).

285

286 In summary, PhyKIT is useful for examining the information content of phylogenomic datasets.  
287 For example, the generation of different phylogenomic data submatrices by selecting subsets of  
288 genes or taxa with certain properties (e.g., retention of genes with the highest numbers of  
289 parsimony-informative sites or following removal of taxa with high long branch scores) can  
290 facilitate the exploration of the robustness of species tree inference or estimating time since  
291 divergence (Salichos and Rokas 2013; Liu *et al.* 2017; Shen *et al.* 2018, 2020; Steenwyk *et al.*  
292 2019; Walker *et al.* 2019; Li *et al.* 2020).

293

#### 294 **A network of gene-gene covariation reveals neighborhoods of genes with shared function**

295 Genes with similar evolutionary histories often have shared functions, are co-expressed, or are  
296 parts of the same multimeric complexes (Sato *et al.* 2005; Clark *et al.* 2012). Using PhyKIT, we  
297 examined gene-gene covariation using 815 genes spanning 1,107 genomes and ~563 million  
298 years of evolution among fungi (Shen *et al.* 2020). By examining 331,705 pairwise combinations  
299 of genes, we found 298 strong signatures of gene-gene covariation (defined as  $r > 0.825$ ). The  
300 two genes with the strongest signatures of covariation were *SEC7* and *TAO3* ( $r = 0.87$ ),  
301 suggesting that their protein products have similar or shared functions. Supporting this  
302 hypothesis, Sec7p contributes to cell-surface growth in the model yeast *Saccharomyces*  
303 *cerevisiae* (Novick and Schekman 1979) and genes with the Sec7 domain are transcriptionally  
304 coregulated with yeast-hyphal switches in the human pathogen *C. albicans* (Song *et al.* 2008).  
305 Similarly, Tao3p in both *S. cerevisiae* and *C. albicans* is part of a RAM signaling network,  
306 which controls hyphal morphogenesis, polarized growth, and cell-cycle related processes  
307 including cell separation, cell proliferation, and phase transitions (Bogomolnaya *et al.* 2006;  
308 Song *et al.* 2008).

309

310 Complex relationships of gene-gene covariation can be visualized as a network (Figure 2).

311 Examination of network neighborhoods identified groups of genes that have shared functions and

312 are parts of the same multimeric complexes. For example, the proteins encoded by *NDC80* and

313 *NUF2* are part of the same kinetochore-associated complex termed the NDC80 complex—which

314 is required for efficient mitosis (Sundin *et al.* 2011)—and significantly covary with one another

315 ( $r = 0.84$ ). Similarly, multiple genes that encode proteins involved in DNA replication and repair

316 (i.e., *POL2*, *MSH6*, *RAD26*, *CDC9*, and *EXO1*) were part of the same network neighborhood,

317 consistent with previous work suggesting an intimate interplay between DNA replication and

318 multiple DNA repair pathways (Tsubouchi and Ogawa 2000; Lujan *et al.* 2012; Boiteux and

319 Jinks-Robertson 2013). Similarly, network neighborhoods of genes involved in ribosome

320 biogenesis, Golgi apparatus-related transport, and control of DNA replication were identified

321 (Figure 2).

322

323 Taken together, these results indicate PhyKIT is a useful tool for evaluating gene-gene

324 covariation and predicting genes' functions (Sato *et al.* 2005; Clark *et al.* 2012; Brunette *et al.*

325 2019). Thus, we anticipate PhyKIT will be helpful for evaluating gene-gene covariation and

326 conducting evolution-based screens for gene functions across the tree of life.

327

### 328 **Identifying polytomies in phylogenomic datasets**

329 Rapid radiations or diversification events have occurred throughout the tree of life (Jarvis *et al.*

330 2014; Liu *et al.* 2017; One Thousand Plant Transcriptomes Initiative 2019; Li *et al.* 2020). One

331 approach to identifying rapid radiations is by testing for the existence of polytomies in species

332 trees (Sayyari and Mirarab 2018; One Thousand Plant Transcriptomes Initiative 2019; Li *et al.*  
333 2020). Polytomies can also arise when the amount of data at hand is insufficient for resolution  
334 (Walsh *et al.* 1999). To demonstrate the utility of PhyKIT to identify polytomies, we tested it  
335 using a simulated set of phylogenies that had a branch whose length was extremely small (Figure  
336 3A). We found that PhyKIT was able to conservatively identify the simulated polytomy. Our  
337 results demonstrate PhyKIT can accurately identify a polytomy and provide further support that  
338 equal support among alternative topologies can be used as a means to identify a rapid radiation.

339

340 We next examined if there is evidence of polytomies in the evolutionary history of filamentous  
341 fungi from the genera *Aspergillus* and *Penicillium*. We examined three branches. The first two  
342 branches—one dating back ~110 million years ago (Figure 3B), and another dating back ~25  
343 million years ago (Figure 3C)—were not polytomies. In contrast, examination of a ~60 million-  
344 year-old branch involving *Lanata-divaricata*, *Citrina*, and *Exilicaulis* (Figure 3D), which are  
345 major lineages (or sections) in the genus *Penicillium*, was consistent with a polytomy. Given the  
346 large number of gene trees used in our analysis (n=1,668), these results are consistent with a  
347 rapid radiation or diversification event in the history of *Penicillium* species.

348

349 In summary, these results suggest that PhyKIT is useful in identifying polytomies in simulated  
350 and empirical datasets. PhyKIT can also be useful for exploring incongruence in phylogenies by  
351 calculating gene support frequencies for alternative topologies. Calculations of gene-based  
352 support for various topologies can be used in diverse applications, including identifying putative  
353 introgression / hybridization events and conducting phylogenetically-based genome-wide  
354 association (PhylogWAS) studies (Pease *et al.* 2016; Steenwyk *et al.* 2019).



355

## 356 **Conclusion**

357 We have developed PhyKIT, a comprehensive toolkit for processing and analyzing MSAs and  
358 trees in phylogenomic datasets. PhyKIT is freely available on GitHub

359 (<https://github.com/JLSteenwyk/PhyKIT>) with extensive documentation and user tutorials

360 (<https://jlsteenwyk.com/PhyKIT>). PhyKIT is a fast and flexible toolkit for the UNIX shell

361 environment, which allows it to be easily integrated into bioinformatic pipelines. We anticipate

362 PhyKIT will be of interest to biologists from diverse disciplines and with varying degrees of

363 experience in analyzing MSAs and phylogenies. In particular, PhyKIT will likely be helpful in

364 addressing one of the greatest challenges in biology, building, understanding, and deriving

365 meaning from the tree of life.

366

## 367 **Data Availability**

368 All data used will become available in figshare (doi: 10.6084/m9.figshare.13118600) upon  
369 publication.

370

## 371 **Acknowledgements**

372 We thank the Rokas lab for helpful discussion and feedback. J.L.S. and A.R. were funded by the

373 Howard Hughes Medical Institute through the James H. Gilliam Fellowships for Advanced

374 Study program. X.X.S. was supported by National Natural Science Foundation of China (No.

375 32071665) and the Fundamental Research Funds for the Central Universities (No.

376 2020QNA6019).

377

378 **References**

- 379 Bogomolnaya L. M., R. Pathak, J. Guo, and M. Polymenis, 2006 Roles of the RAM signaling  
380 network in cell cycle progression in *Saccharomyces cerevisiae*. *Curr. Genet.* 49: 384–92.  
381 <https://doi.org/10.1007/s00294-006-0069-y>
- 382 Boiteux S., and S. Jinks-Robertson, 2013 DNA Repair Mechanisms and the Bypass of DNA  
383 Damage in *Saccharomyces cerevisiae*. *Genetics* 193: 1025–1064.  
384 <https://doi.org/10.1534/genetics.112.145219>
- 385 Brunette G. J., M. A. Jamalruddin, R. A. Baldock, N. L. Clark, and K. A. Bernstein, 2019  
386 Evolution-based screening enables genome-wide prioritization and discovery of DNA repair  
387 genes. *Proc. Natl. Acad. Sci.* 116: 19593–19599. <https://doi.org/10.1073/pnas.1906559116>
- 388 Chen M.-Y., D. Liang, and P. Zhang, 2017 Phylogenomic Resolution of the Phylogeny of  
389 Laurasiatherian Mammals: Exploring Phylogenetic Signals within Coding and Noncoding  
390 Sequences. *Genome Biol. Evol.* 9: 1998–2012. <https://doi.org/10.1093/gbe/evx147>
- 391 Chikina M., J. D. Robinson, and N. L. Clark, 2016 Hundreds of Genes Experienced Convergent  
392 Shifts in Selective Pressure in Marine Mammals. *Mol. Biol. Evol.* 33: 2182–2192.  
393 <https://doi.org/10.1093/molbev/msw112>
- 394 Clark N. L., E. Alani, and C. F. Aquadro, 2012 Evolutionary rate covariation reveals shared  
395 functionality and coexpression of genes. *Genome Res.* 22: 714–720.  
396 <https://doi.org/10.1101/gr.132647.111>
- 397 Cock P. J. A., T. Antao, J. T. Chang, B. A. Chapman, C. J. Cox, *et al.*, 2009 Biopython: freely  
398 available Python tools for computational molecular biology and bioinformatics.  
399 *Bioinformatics* 25: 1422–1423. <https://doi.org/10.1093/bioinformatics/btp163>
- 400 Degnan J. H., and L. A. Salter, 2005 Gene tree distributions under the coalescent process.

- 401 Evolution (N. Y). 59: 24–37. <https://doi.org/10.1111/j.0014-3820.2005.tb00891.x>
- 402 Doolittle W. F., and E. Baptiste, 2007 Pattern pluralism and the Tree of Life hypothesis. Proc.  
403 Natl. Acad. Sci. 104: 2043–2049. <https://doi.org/10.1073/pnas.0610699104>
- 404 Doyle V. P., R. E. Young, G. J. P. Naylor, and J. M. Brown, 2015 Can We Identify Genes with  
405 Increased Phylogenetic Reliability? Syst. Biol. 64: 824–837.  
406 <https://doi.org/10.1093/sysbio/syv041>
- 407 Felsenstein J., 1978 Cases in which Parsimony or Compatibility Methods will be Positively  
408 Misleading. Syst. Biol. 27: 401–410. <https://doi.org/10.1093/sysbio/27.4.401>
- 409 Fourment M., and M. J. Gibbs, 2006 PATRISTIC: a program for calculating patristic distances  
410 and graphically comparing the components of genetic change. BMC Evol. Biol. 6: 1.  
411 <https://doi.org/10.1186/1471-2148-6-1>
- 412 Hunter J. E., and S. H. Cohen, 2007 Package: igraph. Educ. Psychol. Meas.  
413 <https://doi.org/10.1177/001316446902900315>
- 414 Jarvis E. D., S. Mirarab, A. J. Aberer, B. Li, P. Houde, *et al.*, 2014 Whole-genome analyses  
415 resolve early branches in the tree of life of modern birds. Science (80-. ). 346: 1320–1331.  
416 <https://doi.org/10.1126/science.1253451>
- 417 Junier T., and E. M. Zdobnov, 2010 The Newick utilities: high-throughput phylogenetic tree  
418 processing in the UNIX shell. Bioinformatics 26: 1669–1670.  
419 <https://doi.org/10.1093/bioinformatics/btq243>
- 420 Kapli P., Z. Yang, and M. J. Telford, 2020 Phylogenetic tree building in the genomic age. Nat.  
421 Rev. Genet. <https://doi.org/10.1038/s41576-020-0233-0>
- 422 Kück P., and G. C. Longo, 2014 FASconCAT-G: extensive functions for multiple sequence  
423 alignment preparations concerning phylogenetic studies. Front. Zool. 11: 81.

- 424 <https://doi.org/10.1186/s12983-014-0081-x>
- 425 Kumar S., G. Stecher, and K. Tamura, 2016 MEGA7: Molecular Evolutionary Genetics Analysis  
426 Version 7.0 for Bigger Datasets. *Mol. Biol. Evol.* <https://doi.org/10.1093/molbev/msw054>
- 427 Lake J. A., 1991 The order of sequence alignment can bias the selection of tree topology. *Mol.*  
428 *Biol. Evol.* <https://doi.org/10.1093/oxfordjournals.molbev.a040654>
- 429 Lanyon S. M., 1988 The Stochastic Mode of Molecular Evolution: What Consequences for  
430 Systematic Investigations? *Auk* 105: 565–573. <https://doi.org/10.1093/auk/105.3.565>
- 431 Laumer C. E., R. Fernández, S. Lemer, D. Combosch, K. M. Kocot, *et al.*, 2019 Revisiting  
432 metazoan phylogeny with genomic sampling of all phyla. *Proc. R. Soc. B Biol. Sci.* 286:  
433 20190831. <https://doi.org/10.1098/rspb.2019.0831>
- 434 Li Y., J. L. Steenwyk, Y. Chang, Y. Wang, T. Y. James, *et al.*, 2020 A genome-scale phylogeny  
435 of Fungi; insights into early evolution, radiations, and the relationship between taxonomy  
436 and phylogeny. *bioRxiv* 2020.08.23.262857. <https://doi.org/10.1101/2020.08.23.262857>
- 437 Liu L., J. Zhang, F. E. Rheindt, F. Lei, Y. Qu, *et al.*, 2017 Genomic evidence reveals a radiation  
438 of placental mammals uninterrupted by the KPg boundary. *Proc. Natl. Acad. Sci.* 114:  
439 E7282–E7290. <https://doi.org/10.1073/pnas.1616744114>
- 440 Lujan S. A., J. S. Williams, Z. F. Pursell, A. A. Abdulovic-Cui, A. B. Clark, *et al.*, 2012  
441 Mismatch Repair Balances Leading and Lagging Strand DNA Replication Fidelity, (C. E.  
442 Pearson, Ed.). *PLoS Genet.* 8: e1003016. <https://doi.org/10.1371/journal.pgen.1003016>
- 443 Novick P., and R. Schekman, 1979 Secretion and cell-surface growth are blocked in a  
444 temperature-sensitive mutant of *Saccharomyces cerevisiae*. *Proc. Natl. Acad. Sci. U. S. A.*  
445 76: 1858–62. <https://doi.org/10.1073/pnas.76.4.1858>
- 446 One Thousand Plant Transcriptomes Initiative, 2019 One thousand plant transcriptomes and the

- 447 phylogenomics of green plants. *Nature* 574: 679–685. <https://doi.org/10.1038/s41586-019->  
448 1693-2
- 449 Pazos F., and A. Valencia, 2001 Similarity of phylogenetic trees as indicator of protein–protein  
450 interaction. *Protein Eng. Des. Sel.* 14: 609–614. <https://doi.org/10.1093/protein/14.9.609>
- 451 Pease J. B., D. C. Haak, M. W. Hahn, and L. C. Moyle, 2016 Phylogenomics Reveals Three  
452 Sources of Adaptive Variation during a Rapid Radiation, (D. Penny, Ed.). *PLOS Biol.* 14:  
453 e1002379. <https://doi.org/10.1371/journal.pbio.1002379>
- 454 Philippe H., H. Brinkmann, D. V. Lavrov, D. T. J. Littlewood, M. Manuel, *et al.*, 2011 Resolving  
455 Difficult Phylogenetic Questions: Why More Sequences Are Not Enough, (D. Penny, Ed.).  
456 *PLoS Biol.* 9: e1000602. <https://doi.org/10.1371/journal.pbio.1000602>
- 457 Phillips M. J., and D. Penny, 2003 The root of the mammalian tree inferred from whole  
458 mitochondrial genomes. *Mol. Phylogenet. Evol.* 28: 171–185.  
459 [https://doi.org/10.1016/S1055-7903\(03\)00057-5](https://doi.org/10.1016/S1055-7903(03)00057-5)
- 460 Revell L. J., 2012 phytools: an R package for phylogenetic comparative biology (and other  
461 things). *Methods Ecol. Evol.* 3: 217–223. <https://doi.org/10.1111/j.2041->  
462 210X.2011.00169.x
- 463 Robinson D. F., and L. R. Foulds, 1981 Comparison of phylogenetic trees. *Math. Biosci.* 53:  
464 131–147. [https://doi.org/10.1016/0025-5564\(81\)90043-2](https://doi.org/10.1016/0025-5564(81)90043-2)
- 465 Rokas A., and S. B. Carroll, 2006 Bushes in the Tree of Life. *PLoS Biol.* 4: e352.  
466 <https://doi.org/10.1371/journal.pbio.0040352>
- 467 Salichos L., and A. Rokas, 2013 Inferring ancient divergences requires genes with strong  
468 phylogenetic signals. *Nature* 497: 327–331. <https://doi.org/10.1038/nature12130>
- 469 Sang T., and Y. Zhong, 2000 Testing Hybridization Hypotheses Based on Incongruent Gene

- 470 Trees, (R. Olmstead, Ed.). Syst. Biol. 49: 422–434.  
471 <https://doi.org/10.1080/10635159950127321>
- 472 Sato T., Y. Yamanishi, M. Kanehisa, and H. Toh, 2005 The inference of protein-protein  
473 interactions by co-evolutionary analysis is improved by excluding the information about the  
474 phylogenetic relationships. Bioinformatics 21: 3482–3489.  
475 <https://doi.org/10.1093/bioinformatics/bti564>
- 476 Sayyari E., and S. Mirarab, 2018 Testing for Polytomies in Phylogenetic Species Trees Using  
477 Quartet Frequencies. Genes (Basel). 9. <https://doi.org/10.3390/genes9030132>
- 478 Shen X.-X., L. Salichos, and A. Rokas, 2016a A Genome-Scale Investigation of How Sequence,  
479 Function, and Tree-Based Gene Properties Influence Phylogenetic Inference. Genome Biol.  
480 Evol. 8: 2565–2580. <https://doi.org/10.1093/gbe/evw179>
- 481 Shen X.-X., X. Zhou, J. Kominek, C. P. Kurtzman, C. T. Hittinger, *et al.*, 2016b Reconstructing  
482 the Backbone of the Saccharomycotina Yeast Phylogeny Using Genome-Scale Data. G3  
483 Genes|Genomes|Genetics 6: 3927–3939. <https://doi.org/10.1534/g3.116.034744>
- 484 Shen X.-X., D. A. Ofulente, J. Kominek, X. Zhou, J. L. Steenwyk, *et al.*, 2018 Tempo and Mode  
485 of Genome Evolution in the Budding Yeast Subphylum. Cell 175: 1533-1545.e20.  
486 <https://doi.org/10.1016/j.cell.2018.10.023>
- 487 Shen X.-X., J. L. Steenwyk, A. L. Labella, D. A. Ofulente, X. Zhou, *et al.*, 2020 Genome-scale  
488 phylogeny and contrasting modes of genome evolution in the fungal phylum Ascomycota.  
489 bioRxiv. <https://doi.org/10.1101/2020.05.11.088658>
- 490 Smith S. A., J. W. Brown, and J. F. Walker, 2018 So many genes, so little time: A practical  
491 approach to divergence-time estimation in the genomic era, (H. Escriva, Ed.). PLoS One 13:  
492 e0197433. <https://doi.org/10.1371/journal.pone.0197433>

- 493 Song Y., S. A. Cheon, K. E. Lee, S.-Y. Lee, B.-K. Lee, *et al.*, 2008 Role of the RAM network in  
494 cell polarity and hyphal morphogenesis in *Candida albicans*. *Mol. Biol. Cell* 19: 5456–77.  
495 <https://doi.org/10.1091/mbc.e08-03-0272>
- 496 Steenwyk J. L., X.-X. Shen, A. L. Lind, G. H. Goldman, and A. Rokas, 2019 A Robust  
497 Phylogenomic Time Tree for Biotechnologically and Medically Important Fungi in the  
498 Genera *Aspergillus* and *Penicillium*, (J. P. Boyle, Ed.). *MBio* 10.  
499 <https://doi.org/10.1128/mBio.00925-19>
- 500 Steenwyk J. L., T. J. Buida, Y. Li, X.-X. Shen, and A. Rokas, 2020 ClipKIT: a multiple sequence  
501 alignment-trimming algorithm for accurate phylogenomic inference. *bioRxiv*  
502 2020.06.08.140384. <https://doi.org/10.1101/2020.06.08.140384>
- 503 Struck T. H., 2014 TreSpEx--Detection of Misleading Signal in Phylogenetic Reconstructions  
504 Based on Tree Information. *Evol. Bioinforma.* 10: EBO.S14239.  
505 <https://doi.org/10.4137/EBO.S14239>
- 506 Sundin L. J. R., G. J. Guimaraes, and J. G. Deluca, 2011 The NDC80 complex proteins Nuf2 and  
507 Hec1 make distinct contributions to kinetochore-microtubule attachment in mitosis. *Mol.*  
508 *Biol. Cell* 22: 759–68. <https://doi.org/10.1091/mbc.E10-08-0671>
- 509 Talevich E., B. M. Invergo, P. J. Cock, and B. A. Chapman, 2012 Bio.Phylo: A unified toolkit  
510 for processing, analyzing and visualizing phylogenetic trees in Biopython. *BMC*  
511 *Bioinformatics* 13: 209. <https://doi.org/10.1186/1471-2105-13-209>
- 512 Tsubouchi H., and H. Ogawa, 2000 Exo1 Roles for Repair of DNA Double-Strand Breaks and  
513 Meiotic Crossing Over in *Saccharomyces cerevisiae*, (T. D. Fox, Ed.). *Mol. Biol. Cell* 11:  
514 2221–2233. <https://doi.org/10.1091/mbc.11.7.2221>
- 515 Virtanen P., R. Gommers, T. E. Oliphant, M. Haberland, T. Reddy, *et al.*, 2020 SciPy 1.0:

516 fundamental algorithms for scientific computing in Python. Nat. Methods.  
517 <https://doi.org/10.1038/s41592-019-0686-2>

518 Walker J. F., N. Walker-Hale, O. M. Vargas, D. A. Larson, and G. W. Stull, 2019 Characterizing  
519 gene tree conflict in plastome-inferred phylogenies. PeerJ 7: e7747.  
520 <https://doi.org/10.7717/peerj.7747>

521 Walsh H. E., M. G. Kidd, T. Moum, and V. L. Friesen, 1999 Polytomies and the Power of  
522 Phylogenetic Inference. Evolution (N. Y). 53: 932. <https://doi.org/10.2307/2640732>

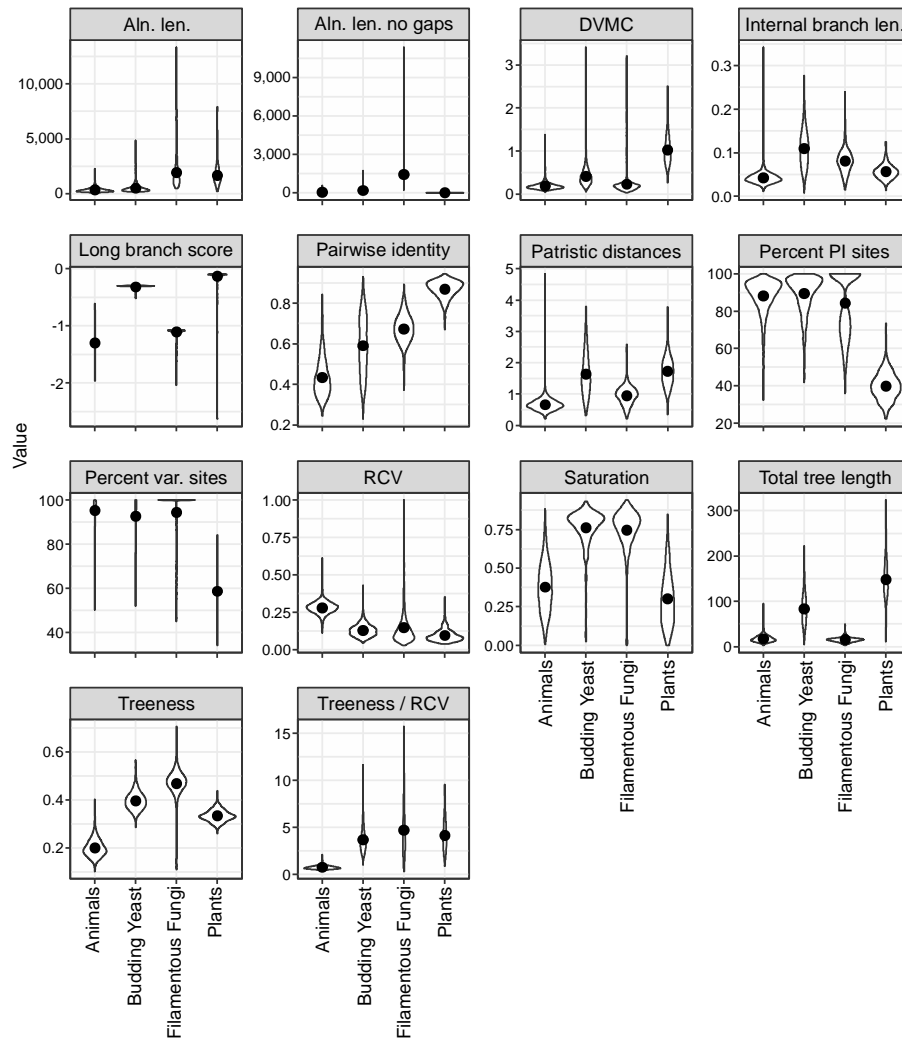
523 Weigert A., C. Helm, M. Meyer, B. Nickel, D. Arendt, *et al.*, 2014 Illuminating the Base of the  
524 Annelid Tree Using Transcriptomics. Mol. Biol. Evol. 31: 1391–1401.  
525 <https://doi.org/10.1093/molbev/msu080>

526 Wolfe N. W., and N. L. Clark, 2015 ERC analysis: web-based inference of gene function via  
527 evolutionary rate covariation: Fig. 1. Bioinformatics btv454.  
528 <https://doi.org/10.1093/bioinformatics/btv454>

529  
530



531



532

533 **Figure 1. Summary of information content in four empirical phylogenomic datasets.** 14

534 metrics implemented in PhyKIT help summarize the information content and identify potential

535 biases in phylogenomic datasets. Each graph displays a violin plot with a black point

536 representing the mean. Error bars indicate one standard error above and below the mean;

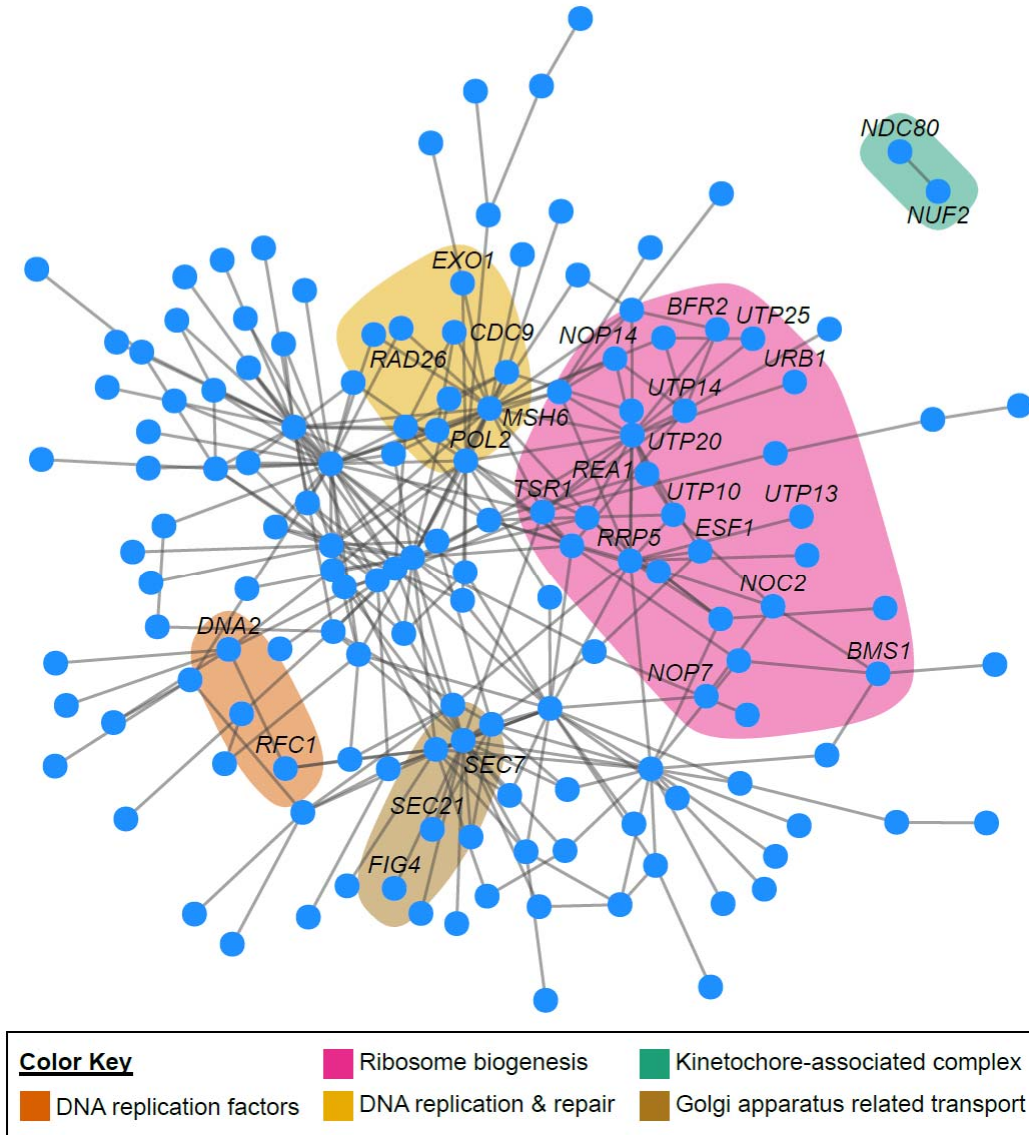
537 however, these are difficult to see in nearly all graphs because they were often near the mean.

538 Abbreviations are as follows: Aln. len.: alignment length; Aln. len. no gaps: alignment length

539 excluding sites with gaps; DVMC: degree of violation of a molecular clock; Internal branch len.:

540 average internal branch length; Patristic distances: average patristic distance in a gene tree;

- 541 Percent PI Sites: percentage of parsimony-informative sites in an MSA; Percent var. sites:  
542 percentage of variable sites in an MSA; RCV: relative composition variability.



543

544 **Figure 2. Gene-gene covariation network inferred from ~550 million years of evolution**

545 **across 1,107 fungi.** A network of significant gene-gene coevolution identifies network

546 neighborhoods representative of associated functional categories. For example, the *NDC80* and

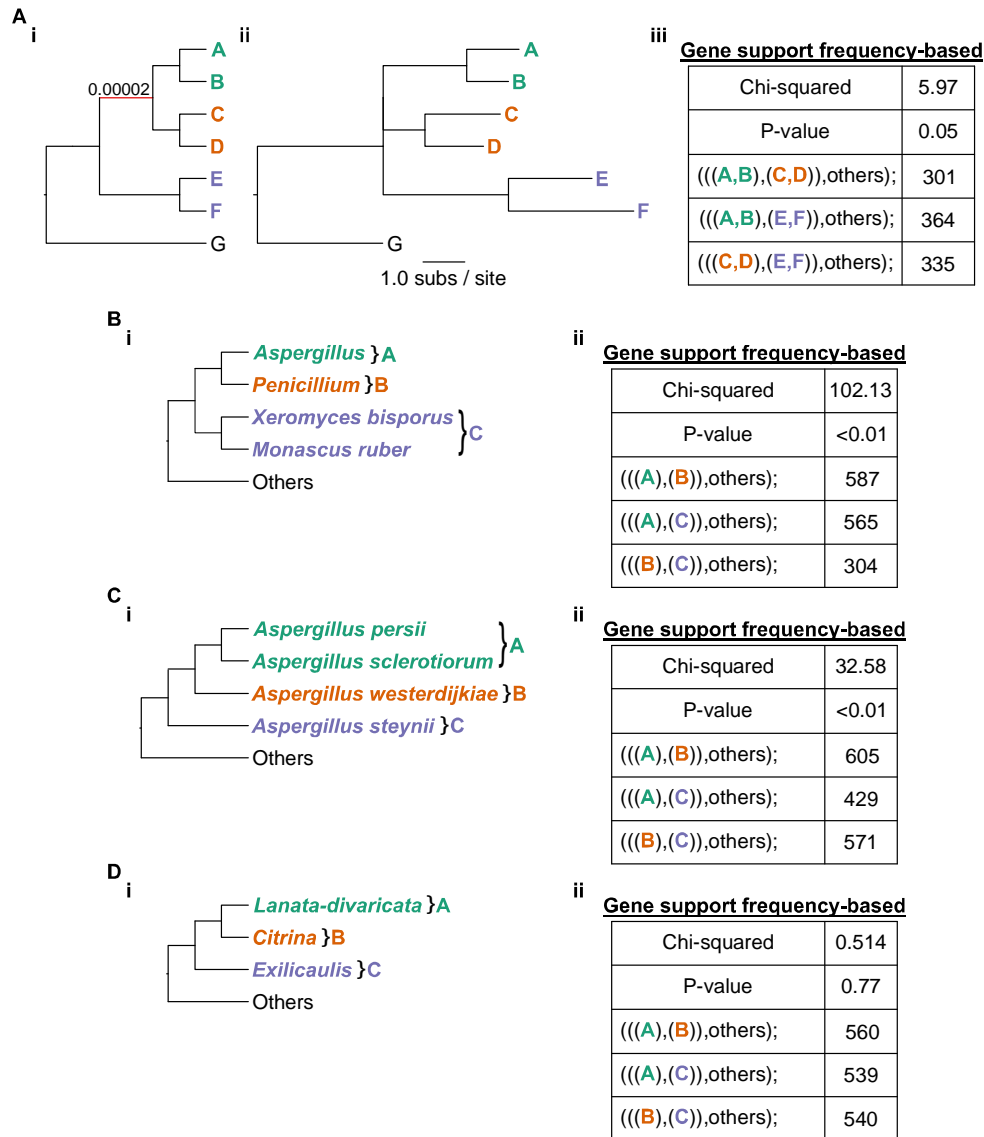
547 *NUF2* genes (toward the top right of the network) were identified to be significantly coevolving

548 with one another ( $r = 0.84$ ,  $p < 0.01$ , Pearson's correlation test); they both encode proteins that

549 are part of the same multimeric kinetochores-associated complex (green). Similarly, genes that are

550 DNA replication factors (orange), contribute to DNA replication and repair processes (yellow),

551 participate in Golgi apparatus-related transport (brown), or ribosome biogenesis (pink) were  
552 found to be neighbors in the network. Network visualization was done with the igraph package,  
553 v1.2.4.2 (Hunter and Cohen 2007), in R, v3.6.2 (<https://www.r-project.org/>).  
554



555

556 **Figure 3. Identifying polytomies from phylogenomic data.** (Ai) A cladogram of a simulated

557 species phylogeny with tip names A-G. The red branch has a very short branch length of  $2 \times 10^{-5}$

558 substitutions per site. (Aii) Phylogram of the same phylogeny shows that all other branches are

559 much longer ( $\geq 1.0$  substitutions per site). (Aiii) After reconstructing the evolutionary history

560 from 1,000 alignments simulated from the phylogeny in Aii, the hypothesis of a polytomy was

561 tested using gene support frequencies for three alternative rooted topologies defined by the

562 clades of green, orange, and purple taxa. Failure to reject the null hypothesis of equal support

563 among genes for each topology is indicative of a polytomy ( $\chi^2 = 5.97$ , p-value = 0.05, Chi-

564 squared test). (B-D) The same approach was then used to examine if there is evidence for a  
565 polytomy at three different branches in a phylogeny of filamentous fungi. (D) Support for a  
566 polytomy ( $\chi^2 = 0.514$ , p-value = 0.77, Chi-squared test) was observed for the relationships  
567 between three different sections of *Penicillium* fungi. These results demonstrate the utility of  
568 gene-support frequencies for evaluating polytomies and examining incongruence in  
569 phylogenomic datasets.  
570

571 **Table 1. Summary of 30 functions implemented in PhyKIT**

<b>Description</b>	<b>Name</b>	<b>Function Alias(es)</b>	<b>Type of function</b>	<b>Input data</b>	<b>Citation</b>
Calculate MSA length	alignment_length	aln_len; al	analytic	alignment	NA
Calculate MSA length after removing sites with gaps	alignment_length_no_gaps	aln_len_no_gaps; alng	analytic	alignment	NA
Combine numerous MSAs into one concatenated matrix	create_concatenation_matrix	create_concat; cc	processing/editing	alignment	NA
Calculate guanine/cytosine content in an MSA	gc_content	gc	analytic	alignment	NA
Calculate summary statistics* for pairwise identity among sequences in an MSA	pairwise_identity	pairwise_id; pi	analytic	alignment	(Chen <i>et al.</i> 2017)
Calculate the number and percentage of parsimony-informative sites in an MSA	parsimony_informative_sites	pis	analytic	alignment	NA
Calculate relative composition variability in an MSA	relative_composition_variability	rel_comp_var; rev	analytic	alignment	(Phillips and Penny 2003)
Rename FASTA entries in an MSA file	rename_fasta_entries	rename_fasta	processing/editing	alignment	NA
Thread DNA sequences over a protein MSA	thread_dna	pal2nal; p2n	processing/editing	alignment	NA
Calculate the number and percentage of variable sites in an MSA	variables_sites	vs	analytic	alignment	NA
Calculate summary statistics* for bipartition support values from a set of phylogenetic trees	bipartition_support_stats	bss	analytic	phylogeny	NA
Multiply all branch lengths of a phylogenetic tree by a specific number	branch_length_multiplier	blm	processing/editing	phylogeny	NA

Collapse bipartitions with bipartition support lower than a user-specified value in a phylogenetic tree	collapse_branches	collapse; cb	processing/editing	phylogeny	NA
Calculates the correlation of evolutionary rates between two genes trees with the same topology	covarying_evolutionary_rates	cover	analytic	phylogeny	(Clark <i>et al.</i> 2012)
Calculate the degree a gene tree violates a molecular clock-like rate of evolution	degree_of_violation_of_a_molecular_clock	dvmc	analytic	phylogeny	(Liu <i>et al.</i> 2017)
Calculate summary statistics* for internal branch lengths in a phylogenetic tree	internal_branch_stats	ibs	analytic	phylogeny	NA
Create numeric labels for bipartitions in a phylogenetic tree	internode_labeler	il	processing/editing	phylogeny	NA
Calculate summary statistics* for long branch scores for taxa in a phylogenetic tree	long_branch_score	lb_score; lbs	analytic	phylogeny	(Weigert <i>et al.</i> 2014)
Calculate the total length of a phylogenetic tree	total_tree_length	tree_len	analytic	phylogeny	NA
Calculate summary statistics* for all patristic distances (or all tip-to-tip distances) in a phylogenetic tree	patristic_distances	pd	analytic	phylogeny	(Fourment and Gibbs 2006)
Use gene support frequencies to test for the existence of a polytomy	polytomy_test	polyt_test; polyt; ptt	analytic	phylogeny	(Sayyari and Mirarab 2018)
Print a phylogenetic tree using ASCII text in the UNIX shell environment	print_tree	print; pt	processing/editing	phylogeny	NA



Prune tips from a phylogenetic tree	prune_tree	prune	processing/editing	phylogeny	NA
Rename tip names in a phylogenetic tree	rename_tree_tips	rename_tree; rename_tips	processing/editing	phylogeny	NA
Calculate raw and normalized Robinson-Foulds distance scores between two phylogenetic trees	robinson_foulds_distance	rf_distance; rf_dist; rf	analytic	phylogeny	(Robinson and Foulds 1981)
Identify putatively spurious sequences by identifying terminal branches with an outlier branch length	spurious_sequence	spurious_seq; ss	analytic	phylogeny	(Jarvis <i>et al.</i> 2014)
Print all tip names in a phylogenetic tree	tip_labels	tree_labels; labels; tl	processing/editing	phylogeny	NA
Calculate treeness or stemminess of a phylogenetic tree	treeness	tness	analytic	phylogeny	(Lanyon 1988)
Calculate saturation, a measure of multiple substitutions across many sites in an MSA	saturation	sat	analytic	alignment and phylogeny	(Philippe <i>et al.</i> 2011)
Calculate treeness divided by relative composition variability, a measure of composition bias susceptibility	treeness_over_rcv	toverr	analytic	alignment and phylogeny	(Phillips and Penny 2003)

572 \*Summary statistics reported are mean, median, 25<sup>th</sup> percentile, 75<sup>th</sup> percentile, minimum, maximum, standard deviation, and variance

573 values. All functions that calculate summary statistics also have verbose options that print out the raw data used to calculate summary

574 statistics.